Conference materials
UDC 524.1
DOI: https://doi.org/10.18721/JPM.161.270

Kinetic modeling of MHD parameters of mildly-relativistic shocks

V.I. Romansky[1]✉, A.M. Bykov[1], S.M. Osipov[1]

[1] Ioffe Institute, St. Petersburg, Russia

✉ romanskyvadim@gmail.com

Abstract. Mildly-relativistic outflows with shocks of velocities 0.1—0.7c were deduced from multiwavelength observations of powerful fast transient sources. These outflows are associated with merging relativistic objects, relativistic supernovae and fast blue optical transients. Relativistic magneto-hydrodynamic (RMHD) models of these objects rely on the equation of state of the fluid, which is a collisionless plasma with a contribution of non-thermal components. In this paper, we present kinetic simulations of mildly-relativistic shocks with Particle-in-Cell and Monte-Carlo techniques to derive the adiabatic index of plasma in the shock downstream directly from the particle distributions, which can be implemented into the RMHD models.

Keywords: cosmic rays, shock, MHD, Particle-in-Cell, Monte-Carlo

Funding: Modeling by V.I. Romansky and A.M. Bykov at RAS JSCC were supported by RSF grant 21-72-20020. Data analysis by S.M. Osipov was supported by 0040-2019-0025 at Ioffe Institute.

Citation: Romansky V.I., Bykov A.M., Osipov S.M., Kinetic modeling of MHD parameters of mildly-relativistic shocks, St. Petersburg State Polytechnical University Journal. Physics and Mathematics. 16 (1.2) (2023) 461—466. DOI: https://doi.org/10.18721/JPM.161.270

Материалы конференции
УДК 524.1
DOI: https://doi.org/10.18721/JPM.161.270

Кинетическое моделирование МГД параметров субрелятивистских ударных волн

В.И. Романский[1]✉, А.М. Быков[1], С.М. Осипов[1]

[1] Физико-технический институт им. А.Ф. Иоффе РАН, Санкт-Петербург, Россия

✉ romanskyvadim@gmail.com

Аннотация. Субрелятивистские ударные волны со скоростями 0.1—0.7c обнаружены в мощных транзиентных объектах. Релятивистские магнитогидродинамические модели таких течений используют уравнение состояния вещества при наличии нетепловой компоненты. В этой работе представлены результаты вычисления показателя адиабаты плазмы за фронтом ударной волны с помощью Particle-in-Cell и Монте-Карло моделирования.

Ключевые слова: космические лучи, ударные волны, МГД, Particle-in-Cell, Монте-Карло

Финансирование: Расчеты Романского В.И. и Быкова А.М. на МСЦ РАН поддержаны грантом РНФ 21-72-20020 Работа Осипова С.М. выполнена в рамках Государственного задания 0040-2019-0025 ФТИ им. Иоффе.

Ссылка для цитирования: Романский В.И., Быков А.М., Осипов С.М. Кинетическое моделирование МГД параметров субрелятивистских ударных волн // Научно-технические ведомости СПбГПУ. Физико-математические науки. 2023. Т. 16. № 1.2. С. 461—466. DOI: https://doi.org/10.18721/JPM.161.270

Introduction

Recent multiwavelength observations of fast energetic transient sources associated with some classes of supernova and neutron star mergers revealed a presence there of mildly-relativistic outflows with shock waves of velocities faster than 0.1c [1–8]. Analysis of 42 daytimescale-evolving transients detected with Zwicky Transient Facility (ZTF) [9] suggested that most of these objects are likely associated with core-collapse supernovae (SNe). The authors distinguished a few sub-types of the typical events as (i) subluminous SNe of Type Ib or IIb; (ii) luminous Type Ibn or hybrid IIn/Ibn SNe; and (iii) short-duration radio-loud luminous events which prototype is nearby AT2018cow event. While the subluminous SNe events of Type IIb are the most numerous, the AT2018cow like events rate is less than 0.1% of the local corecollapse SNe rate [9]. The multiwavelength data on fast SNe related transients can be generally understood assuming an action of a powerful central engine in the collapsing stars which can launch a relativistic jet-type outflow. The relativistic hydrodynamical simulations performed in [10, 11] illustrated that depending on the time duration of the central engine power activity either a GRB type jet source (for a long enough activity time) or, for a shorter power injection time, a somewhat broader outflow and a radio bright relativistic SN can be produced by a collapsing star. The different energy injection regimes by the central engine result in different energy versus the ejecta speed distributions. The powerful jet breaking through the stellar envelope can form a mildly-relativistic expanding cocoon containing the energy ~10^{51} ergs (see e.g. [12]). The cocoon interacting with the circumstellar winds may emit the synchrotron self-absorbed radio emission observed in the fast optical transients [13]. The physical models of particle acceleration in the fast transients based on the particle in cell simulations of mildly-relativistic shocks in barionic plasma produced by the central engine activity in the fast transients were discussed in [14]. Mildly-relativistic shocks are also determining the transition from the early highly-relativistic to the later time semi-relativistic likely barion-dominated outflows in the gamma-ray burst afterglows (see e.g. [15–17]) where the models can be used to model the non-thermal radiation. Moreover, mildly-relativistic shocks in stellar mass transient sources can be considered as efficient accelerators of cosmic rays well above PeV regime (see [18] and the references therein). The future Large Synoptic Survey Telescope will detect a large amount of fast transients providing good possibilities to of the follow up multiwavelength studies. Therefore, there is a clear need in detailed modeling of different appearances of the semi-relativistic outflows in the transient sources. While to model the global structure of the flows the RMHD simulations are widely used, the collisionless shocks need the microscopic kinetic type of simulations since the collisionless shocks are producing non-thermal components which may influence the equation of state and the macroscopic parameters like the adiabatic indexes of the semi-relativistic plasma. Therefore, we present below the results of simulations of the macroscopic plasma parameters, which can be used in the global RMHD simulations.

Particle-in-Cell simulations

In this work, we use the particle-in-cell code Smilei [19] for modeling collisionless shocks. The simulation domain is two-dimensional with the reflective wall on the left boundary along the x-axis and the plasma flowing in through the right boundary. The boundary conditions along the y-axis are periodic.

The simulation parameters are: the initial flow Lorentz factor Γ is in interval 1.05–1.5 for different setups, the flow magnetization

$$\sigma = \frac{B^2}{4\pi\Gamma n_0 (m_p + m_e)c^2} = 0.0002,$$

where B is the magnetic field, m_p and m_e are proton and electron masses, c is speed of light. The upstream number density n_0 is equal to 1, but all quantities can be easily scaled to different value. The temperature $T = 0.02$ in units of the electron rest energy and the electron mass is increased up to $m_e = m_p/100$. We used setups with different velocities of plasma flow $v_u = \beta_u c$ and inclination angles of magnetic field: ϑ is angle between the magnetic field and the flow velocity and φ is angle of field rotation in perpendicular plane, $\varphi = 0$ corresponds to the magnetic field lying in the simulation plane. Setups and their parameters are listed in Table 2.

The spatial grid step is $dx = 0.2c/\omega_p$ and the time step $dt = 0.1/\omega_p$, where

$$\omega_p = \sqrt{\frac{4\pi n_0 e^2}{m_e}}$$

is the plasma frequency, e is the absolute value of the electron charge. The size of the simulation box along the x-axis is $L_x = 40000c/\omega_p$ and in the transverse direction $L_y = 100c/\omega_p$. These scales correspond to 200000 and 500 grid points in x and y directions, respectively.

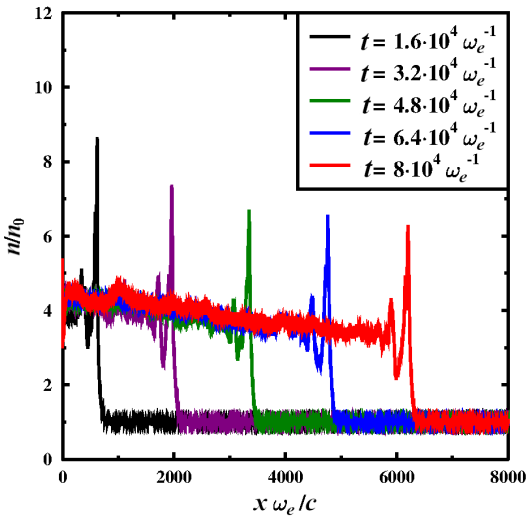

Fig. 1. Time evolution of number density normalized to the far upstream number density in setup B30

We obtain the MHD parameters of the shock from the simulation. The position of the shock front is well defined as shown in Fig. 1 so we can evaluate the shock velocity in the downstream frame v^d_{sh} and $\beta^d_{sh} = v^d_{sh}/c$ The shock velocity in the upstream frame is defined as $\beta_{sh} = (\beta_u + \beta^d_{sh})/(1 + \beta_u \cdot \beta^d_{sh})$ We can find temperature of each particle species behind the shock, minimizing the functional

$$f(T) = \int_{mc^2}^{5mc^2} (F(E) - F_{mj}(E,T))^2 dE,$$

where $F(E)$ is simulated distribution function and $F_{mj}(E,T)$ is Maxwell-Juttner distribution function. Fitting of distribution function is shown in Fig. 2. Also on can see non-thermal tail of distribution, which is cut at level $F(E) \approx 10^{-7}$ to avoid strong statistical fluctuations at high energies. Also, we can derive adiabatic index for every species of particles using definition $\gamma_i = 1 + P/E_k$ where P is the pressure and E_k is the kinetic energy of particles in the plasma rest frame.

$$P = \int F(E) v_x(E,\vartheta) p_x(E,\vartheta) 2\pi \sin(\vartheta) d\vartheta dE\,,$$

$$\text{and } E_k = \int F(E)(E - mc^2) 2\pi \sin(\vartheta) d\vartheta dE.$$

Also we define $\hat{\gamma}-$ the adiabatic index, evaluated with the same formulae but using the Maxwell-Juttner particle distribution with the corresponding temperature.

Table 1

Parameters of setups

Setup	ϑ	φ	β_u	β^d_{sh}	β_{sh}	γ_p	γ_e	$T_p\ 10^{10}$K	$T_e\ 10^{10}$K	$\hat{\gamma}_p(T_p)$	$\hat{\gamma}_e(T_e)$
A30	30	90	0.5	0.13	0.59	1.620	1.389	75.5	19.0	1.617	1.389
A80	80	90	0.5	0.16	0.61	1.601	1.396	54.7	16.3	1.629	1.397
B30	30	90	0.3	0.088	0.38	1.647	1.499	14.5	4.0	1.656	1.502
B50	50	90	0.3	0.098	0.39	1.648	1.468	11.0	5.9	1.658	1.469
C30	30	0	0.3	0.088	0.38	1.647	1.502	14.4	3.9	1.656	1.504
D30	30	90	0.1	0.035	0.135	1.665	1.574	1.9	1.3	1.665	1.589
D80	80	90	0.1	0.052	0.151	1.664	1.580	2.6	1.5	1.665	1.579

Notations: ϑ and φ are orientation angles of magnetic field, β_u is upstream velocity in units of c, β^d_{sh} is shock velocity in downstream (laboratory) frame, β_{sh} is shock velocity in upstream frame, γ_p and γ_e are protons and electrons adiabatic indices, T_p and T_e are temperatures of Maxwellian part of distribution and $\hat{\gamma}_p(T_p)$ and $\hat{\gamma}_e(T_e)$ are adiabatic indices, evaluated for Maxwell-Juttner distribution with corresponding temperature.

One can see from Table 1 that the adiabatic index obtained from PIC simulation is smaller than obtained from the simple hydrodynamic theory. It should be taken into account in the MHD simulations. This difference increases when the particle acceleration is more efficient (case of the quasi-parallel shock). Also, the PIC simulation cannot simulate long non-thermal tales of distributions because of it is high computational cost, and other methods, such as hybrid and Monte-Carlo simulation are needed for more precise modeling of the MHD parameters.

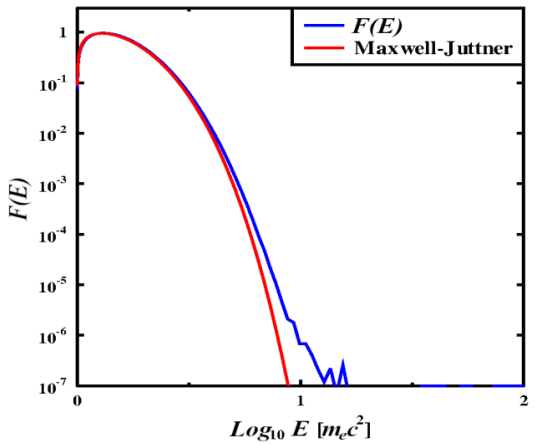

Fig. 2. Fit of the electron distribution in the shock downstream with Maxwell-Juttner distribution, setup B30

Monte-Carlo simulation

Due to the limited computing power, PIC modeling can be performed only in a small area of the volume of real astrophysical objects. To describe astrophysical objects on their real scales, it is necessary to involve other numerical models. One of such models is the Monte Carlo calculations, which, unlike the PIC calculations, require the introduction of phenomenological laws, such as the mean free path of particles, the growth rates of plasma instabilities.

We develop a nonlinear numerical stationary plane-parallel relativistic Monte Carlo model of particle acceleration by longitudinal collisionless shocks [14]. Particle acceleration occurs by the first-order Fermi mechanism. The particles are scattered by the magnetic fluctuations and repeatedly cross the shock front. In our model, based on an iterative scheme, the conservation laws of energy and momentum fluxes near the shock are fulfilled. The model takes into account the modification of the upstream by the pressure of accelerated particles, the amplification of the magnetic fluctuations due to plasma instabilities caused by the anisotropy of the accelerated particle distribution function in the upstream, the dissipation of turbulent modes, and the turbulent cascade. Particle propagation is organized based on pitch-angle scattering. The particles are divided into accelerated and background. The particle is considered as accelerated if it has crossed the front of the shock at least once from the downstream to the upstream.

Table 2 shows the results of Monte Carlo calculations for different shock velocities $v_{sh} = \beta_{sh} c \cdot \gamma_{th}$, γ_{cr}, γ_{tot} are the adiabatic indices of the background plasma, the accelerated particle distribution and the total in the downstream, respectively. T_{th} is the temperature of background protons in the downstream. Other model parameters except v_{sh} are the same in all calculations. The free escape boundary of particles is at the coordinate $x_{FEB} = -10 \cdot 5^{14}$ cm, the shock front corresponds to the coordinate $x = 0$. The number density of the background plasma $n_0 = 5 \cdot 10^5$ cm^{-3} in the far unperturbed upstream. The rms turbulent magnetic field $B_{st}(x_{FEB})$ is equal to the constant magnetic field $B_0 = 3 \cdot 10^{-3} G$ in the far unperturbed upstream.

$$B(x) = \sqrt{B_{st}^2(x) + B_0^2} \ .$$

Table 2

Results of Monte Carlo calculations

Setup	β_{sh}	γ_{th}	γ_{cr}	γ_{tot}	$T_{th}\, 10^{10} K$
MC1	0.1	1.66	1.43	1.49	0.59
MC2	0.3	1.66	1.42	1.49	7.11
MC3	0.5	1.64	1.41	1.49	26.5
MC4	0.7	1.61	1.40	1.48	82.4

Notations: β_{sh} is shock velocity in upstream frame in units of c, γ_{th} is adiabatic index of background plasma, γ_{cr} is adiabatic index of accelerated particles, γ_{tot} is total adiabatic index and T_{th} is a temperature of background plasma.

Fig. 3 shows the profiles of the background plasma flow velocity and the magnetic field. The turbulent part of the magnetic field is amplified due to plasma instabilities and adiabatically. $r_{g0} = m_p c v_{sh}/eB_0$, where e is elementary charge.

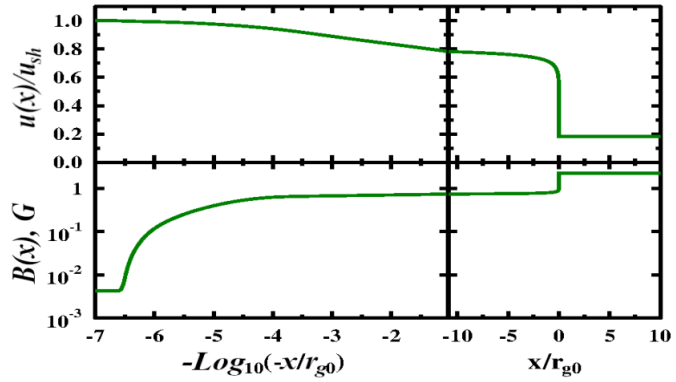

Fig 3. Background plasma velocity profile (upper panel) and magnetic field profile (bottom panel) for the Monte Carlo calculation MC1. Coordinate is shown in units of $r_{g0} = m_p c v_{sh}/eB_0$, where e is elementary charge

The scales achievable in PIC modeling are of the order of several r_{g0}, so the PIC modeling can describe a small area near the shock compared to the Monte Carlo modeling (see Fig. 3). Since the maximum energies of accelerated particles strongly depend on the size of the system, in the Monte Carlo calculations, the maximum energies of particles are many orders of magnitude higher than in the PIC calculations. The temperature of the background plasma in the downstream in the Monte Carlo simulation is also affected by the amplification of modes by plasma instabilities associated with the anisotropy of the distribution of the high-energy accelerated particles and the energy dissipation of these modes at the upstream scales.

Conclusions

Hydrodynamic and RMHD models are constructed to interpret the light-curves and spectra of fast transients (e.g. [20, 10, 5, 21, 22, 13, 23] and the reference therein). Results of kinetic modeling of mildly-relativistic shocks show that adiabatic index of plasma differs from typical values, which are usually used in hydrodynamic models, due to non maxwellian distribution of particles. It should be taken into account during MHD modeling of global structures of mildly-relativistic outflows. Also, Particle-in-Cell modeling provides electrons temperature, which can be useful for hydrodynamic and hybrid modeling.

Acknowledgments

Modeling by V.I. Romansky and A.M.Bykov at RAS JSCC were supported by RSF grant 21-72-20020. Data analysis by S.M.Osipov were supported by 0040-2019-0025 at Ioffe Institute. Some results of the work were obtained using computational resources of Peter the Great St. Petersburg Polytechnic University Supercomputing Center (http://scc.spbstu.ru).

REFERENCES

1. **Arcavi I., Wolf W.M., Howell D.A., et al.,** Rapidly Rising Transients in the Supernova—Superluminous Supernova Ga, Astrophysical Journal 819 (2016) 35.

2. **Margutti R., Metzger B.D., Chornock R., et al.,** An Embedded X-Ray Source Shines through the Aspherical AT 2018cow: Revealing the Inner Workings of the Most Luminous Fast-evolving Optical Transients, Astrophysical Journal 872 (2019) 18.

3. **Ho A. Y.Q., Perley D.A., Kulkarni S.R., et al.,** The Koala: A Fast Blue Optical Transient with Luminous Radio Emission from a Starburst Dwarf Galaxy at z = 0.27, Astrophysical Journal 895 (2020) 49.

4. **Nayana A.J., Chandra P.,** uGMRT Observations of a Fast and Blue Optical Transient—AT 2018cow, Astrophysical Journal Letters 912 (2021) L9.

5. **Metzger B.D.,** Kilonovae, Living Reviews in Relativity 23 (2019) 1.
6. **Margutti R., Chornock R.,** First Multimessenger Observations of a Neutron Star Merger, Annual Review of Astronomy and Astrophysics 59 (2021) pp. 155–202.
7. **Kremer K., Lu W., Piro A. L., et al.,** Fast Optical Transients from Stellar-mass Black Hole Tidal Disruption Events in Young Star Clusters, Astrophysical Journal 911 (2021) 104.
8. **Hajela A., Margutti R., Bright J. S., et al.,** Evidence for X-Ray Emission in Excess to the Jet-afterglow Decay 3.5 yr after the Binary Neutron Star Merger GW 170817: A New Emission Component, Astrophysical Journal Letters 927 (2022) L17.
9. **Ho A.Y.Q., Perley D. A., Gal-Yam A., et al.,** The Photometric and Spectroscopic Evolution of Rapidly Evolving Extragalactic Transients in ZTF *arXiv e-prints* arXiv:2105.08811 (2021).
10. **Lazzati D., Morsony B.J., Blackwell C.H., Begelman M.C.,** Unifying the Zoo of Jet-driven Stellar Explosions, Astrophysical Journal 750 (2012) 68.
11. **Corsi A., Lazzati D.,** Gamma-ray burst jets in supernovae, New Astronomy Reviews 92 (2021) 101614.
12. **Piran T., Nakar E., Mazzali P., Pian E.,** Relativistic Jets in Core-collapse Supernovae, Astrophysical Journal Letters 871 (2019) L25.
13. **Gottlieb O., Tchekhovskoy A., Margutti R.,** Shocked jets in CCSNe can power the zoo of fast blue optical transients, Monthly Notices of the Royal Astronomical Society 513 (2022) pp. 3810–3817.
14. **Bykov A., Romansky V., Osipov S.,** Particle Acceleration in Mildly Relativistic Outflows of Fast Energetic Transient Sources, Universe 8 (2022) 32.
15. **Piran T.,** The physics of gamma-ray bursts, Reviews of Modern Pysics 76 (2004) 1143.
16. **Mreszraros P.,** Gamma-ray bursts, Reports on Progress in Physics 69 (2006) 2259–2321.
17. **van Eerten H., van der Horst A., MacFadyen A.,** Gamma-Ray Burst Afterglow Broadband Fitting Based Directly on Hydrodynamics Simulations, Astrophysical Journal 749 (2012) 44.
18. **Bykov A.M., Ellison D.C., Marcowith A., Osipov S. M.,** Cosmic Ray Production in Supernovae, Space Science Reviews 214 (2018) 41.
19. **Derouillat J., Beck A., Prerez F., et al.,** SMILEI: A collaborative, open-source, multi-purpose particle-in-cell code for plasma simulation, Computer Physics Communications 222 (2018) 351–373.
20. **Matzner C.D., McKee C.F.,** The Expulsion of Stellar Envelopes in Core-Collapse Supernovae, Astrophysical Journal 510 (1999) pp. 379–403.
21. **Leung S.C., Blinnikov S., Nomoto K., et al.,** A Model for the Fast Blue Optical Transient AT2018cow: Circumstellar Interaction of a Pulsational Pair-instability Supernova, Astrophysical Journal 903 (2020) 66.
22. **Urvachev E., Shidlovski D., Tominaga N., Glazyrin S., Blinnikov S.,** The Simulation of Superluminous Supernovae Using the M1 Approach for Radiation Transfer, Astrophysical Journal Supplement Series 256 (2021) 8.
23. **Eisenberg M., Gottlieb O., Nakar E.,** Observational signatures of stellar explosions driven by relativistic jets, Monthly Notices of the Royal Astronomical Society 517 (2022) 582.

THE AUTHORS

ROMANSKY Vadim I.
romanskyvadim@gmail.com
ORCID: 0000-0003-1863-2957

BYKOV Andrei M.
byk@astro.ioffe.ru
ORCID: 0000-0003-0037-2288

OSIPOV Sergei M.
osm2004@mail.ru
ORCID: 0000-0001-8806-0259

Received 28.10.2022. Approved after reviewing 08.11.2022. Accepted 16.11.2022.